

# Design and performance analysis of PIN-type photodetector with optimized Schottky contact

Zhen Zhao

*School of Electronic Information and Electrical Engineering, Changsha University, Changsha, 410022, China*

**Abstract:** *In this paper, the study designs a multi-layer MoS<sub>2</sub>/Ge heterojunction PIN photodetector, capitalizing on the high absorptivity and tunable bandgap properties of the two-dimensional material MoS<sub>2</sub>. To mitigate dark current and minimize noise, a Schottky contact is incorporated into the photodetector, enhancing its detection capabilities. The device's performance parameters were simulated using Silvaco TCAD software. The results indicate a dark current as low as  $1.27 \times 10^{-19}$  A and a photocurrent reaching  $10^{-7}$  A. The device exhibits stable responses across ultraviolet, visible, and infrared spectra. The transient response analysis reveals a rise time of 1.6 microseconds and a fall time of 1.1 microseconds, with an optical modulation frequency of 500 MHz and an operating bandwidth of up to 23.4 GHz. These characteristics confirm the photodetector's capability for stable operation in ultrafast light detection scenarios. Additionally, the noise equivalent power of the photodetector reaches an impressive  $10^{-18}$  W/Hz<sup>0.5</sup>, which is  $10^{12}$  Jones higher than conventional detectors, underscoring the MoS<sub>2</sub>/Ge heterojunction photodetector's significant potential for applications in low-light and ultrafine light detection scenarios.*

**Keywords:** *MoS<sub>2</sub>, Heterojunction Photodetector, Schottky contact, Transient response*

## 1. Introduction

With the development of science and technology and the advent of the information age, photodetector, as an important photodetector, is widely used in optical communication. With the advent of the intelligent era, people's growing demand continues to expand, and photoelectric detectability with wide spectrum, high detectability and high responsiveness is imminent.[1]At present, most photodetectors have a short response band, are strictly limited to ultraviolet or infrared band detection, and require a strict working environment.[1] Some infrared photodetectors are made of bandgap semiconductors such as Ge,HgCdTe, etc, which have high cost and strict working environment requirements.[2] As a result, the photodetector is at an impasse.

The birth of graphene broke the deadlock, and the layered two-dimensional material with high light absorption and high carrier mobility began to attract much attention in optoelectronics.[3-4] Therefore, two-dimensional supermetallic sulfides have become popular materials. Molybdenum disulfide is a typical representative, and its single or multilayer MoS<sub>2</sub> has a strong absorption effect on light.[5-7] Due to its bandgap variability, MoS<sub>2</sub>'s photodetectors have a wide range of light detection capabilities. Due to the inertness of the sulfide surface, the dark current of the photodetector can be reduced. The MoS<sub>2</sub> photodetector can also detect at room temperature, and the operating environment is not strict. For the above reasons, the two-dimensional material MoS<sub>2</sub> is widely used in photodetectors.

In this paper, a multi-layer molybdenum disulfide heterojunction photodetector is designed and simulated by taking advantage of the wide spectral response range and fast response speed of molybdenum disulfide, which improves the performance of the photodetector and provides theoretical guidance for the specific application of the photodetector.

## 2. PIN type photodetector design

### 2.1 Principle of PIN photodiode

The PIN type photodiode is essentially a reverse bias photodiode, which is based on the PN junction structure and adds a layer of low-clutter or no-clutter intrinsic layer in the middle. The principle of its

operation in the case of reverse bias is shown in the Figure 1.

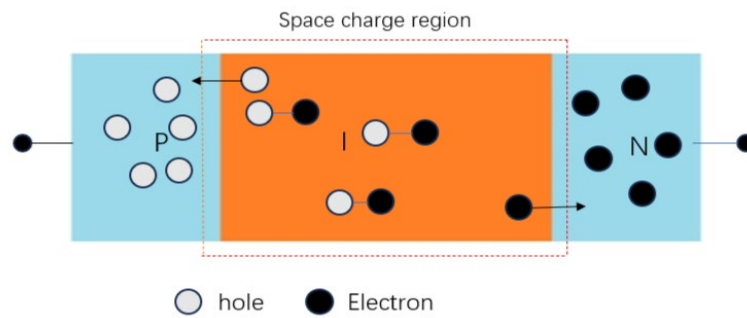


Figure 1: PIN schematic diagram

Assuming that region I is a low P-type hybrid, in the absence of bias, region I and region N will form a PN junction. In the case of reverse bias, the space charge region of region I and region N will widen under the action of external electric field and built-in electric field. When the external voltage increases to a certain value, the space charge region of region I will completely form under the action of diffusion and drift, and the space charge region will widen, which improves the absorption of light. The carrier diffusion time is shortened, the response speed is obviously accelerated, and the responsivity of the photodiode is improved.

The principle of PIN-type photodiode can be explained by means of a band diagram, as shown in Figure 2.

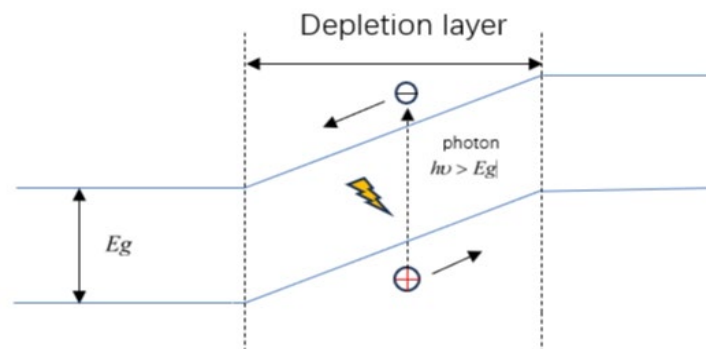


Figure 2: Band diagram of PIN-type photodiode

When the incident light illuminates the photosensitive surface, its energy is absorbed by electrons in the photosensitive material. When the energy of the incident photon is greater than the band gap width, electrons in the valence band can absorb the photon energy and transition to the conduction band, thus forming an electron-hole pair and forming holes in the valence band. When the photodiode is in the case of reverse bias, the carrier drifts, forming an electric current.

## 2.2 Structural design of photodetector

In this paper, the device structure modeling and device characteristic simulation of PIN-type MoS<sub>2</sub>/Ge heterojunction photodetector are carried out based on Silvaco Atlas. Figure 3 is the device structure diagram of the photodetector.

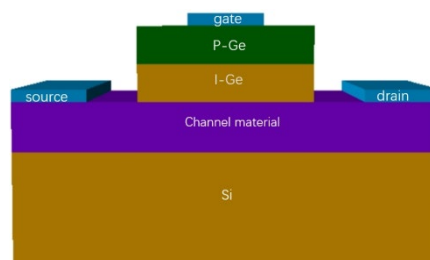


Figure 3: Device structure diagram

The structure uses Si with a thickness of 0.35  $\mu\text{m}$  as the substrate, and on top of the substrate is an inverted PIN structure of MoS<sub>2</sub>/I-Ge/P-Ge. Among them, the channel material above the substrate uses 5 layers of MoS<sub>2</sub>, with a total thickness of 0.2  $\mu\text{m}$ . The thickness of P-Ge layer in PIN structure is, and the method of low clutter is adopted. The I-Ge of the middle layer adopts the thickness of is and the low impurity is adopted. The electrode on the left side of the channel material is copper as a Schott group, which forms a Schottky contact with the channel material, and the electrode on the right side of the channel material is titanium as a drain material. The distance between the source/drain electrodes and I-Ge is 0.5 microns to avoid edge effect.

In this paper, the custom material function of ATLAS is used to model MoS<sub>2</sub>. Based on the self-hybrid effect of MoS<sub>2</sub>, the hybrid is incorporated on the basis of polycrystalline silicon. Table 1 shows the material parameters of MoS<sub>2</sub>.

*Table 1: Material parameters of MoS<sub>2</sub>*

Material parameters of MoS <sub>2</sub>	Numerical value
Band-gap width	1.3 eV
dielectric constant	7.82
electron affinity	4 eV
channel impurity concentration	$1.5 \times 10^{17} \text{ cm}^{-3}$
conduction band density	$5 \times 10^{19} \text{ cm}^{-3}$
valence band density	$8 \times 10^{19} \text{ cm}^{-3}$

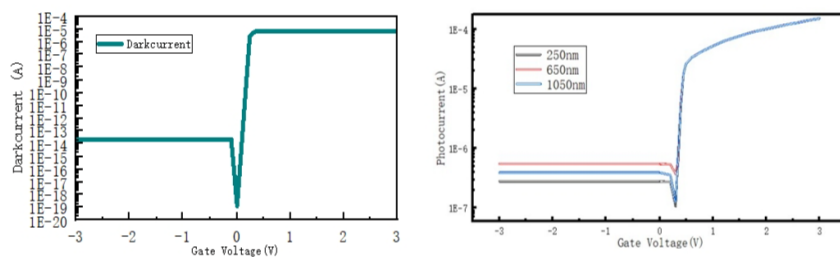
### 3. Simulation and analysis of photodetector

#### 3.1 I-V characteristic curve

Figure4 (a) is the dark current curve obtained by the linear increase of the gate voltage of the photodetector from -3V to 3V. It can be seen from the figure that the dark current of the detector at 0 bias voltage is  $1.27 \times 10^{-19}$  A. The dark current has good rectification effect in the voltage range and has a rectification ratio of more than  $10^8$ , indicating that MoS<sub>2</sub> and Ge form a good heterojunction.

Figure4 (b) shows the photocurrent curves of the photodetector at different wavelengths. The curve is a photocurrent curve with incident power of 0.1  $\mu\text{w}$  and wavelength of 250 nm,650 nm and 1050 nm. It can be seen from the curve that there is a rectification ratio of more than 100 times in this bias range. In the case of 0 bias voltage, the photocurrent can reach the order of  $10^{-7}$  at least, which is much higher than the dark current, which indicates that the photodetector has a good photoelectric detection ability and can effectively avoid the influence of dark current.

In order to explore the degree of dependence of photocurrent on optical power, we studied the photocurrent of the photodetector under different optical power at 0 bias and wavelength of 250 nm and 650 nm respectively. Figure4 (c) shows the photocurrent of the photodetector with a wavelength of 250 nm under different input optical power at 0 bias. Among them, at 0.25  $\mu\text{w}$ , 0.5  $\mu\text{w}$ , 0.75  $\mu\text{w}$ , 1  $\mu\text{w}$  power corresponding photocurrent is  $6.9 \times 10^{-7}$  A;  $1.38 \times 10^{-6}$  A;  $2.07 \times 10^{-6}$  A;  $2.76 \times 10^{-6}$  A. Figure4 (d) is the photocurrent of the photodetector with a wavelength of 250 nm at different input optical power at 0 bias. Among them, the corresponding photocurrent at 0.25  $\mu\text{w}$ , 0.5  $\mu\text{w}$ , 0.75  $\mu\text{w}$ , 1  $\mu\text{w}$  power is  $7.0 \times 10^{-7}$  A;  $1.401 \times 10^{-6}$  A.;  $2.102 \times 10^{-6}$  A;  $2.802 \times 10^{-6}$  A. According to figure4 (c) and figure4 (d), the photocurrent increases with the increase of optical power. In the case of positive bias, the photocurrent increases rapidly with the increase of positive bias, and the contribution of optical power to the photocurrent is not great. Moreover, the minimum photocurrent shifts to the right with the increase of optical power.



(a) Dark current curve      (b) Photocurrent curves at different wavelengths

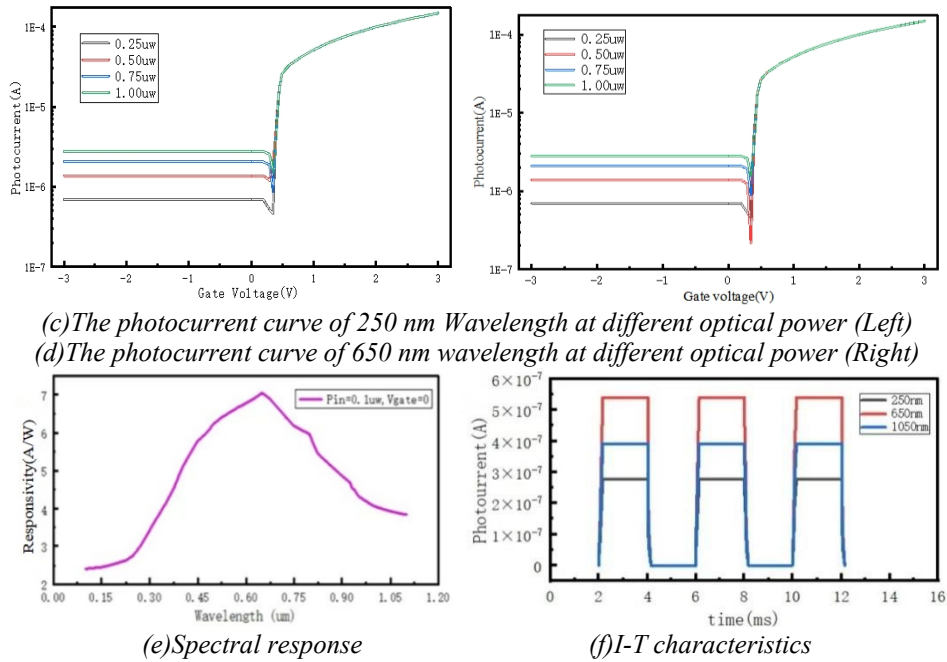


Figure 4: Photoelectric characteristic of PIN photodetector

In order to study the relationship between photocurrent and time dependence of photodetector, i.e. I-T curve. We investigate the I-T curve of the photodetector at different wavelengths. Figure 4 (f) shows the photocurrent curve obtained when the detector operates at 0 bias voltage and the incident light power is 0.1 uW. At different wavelengths, the optical signal is cut off/input every 2 ms. The corresponding photocurrents of 250 nm, 650 nm and 1050 nm are  $2.72 \times 10^{-7}$  A respectively.  $5.42 \times 10^{-7}$  A.  $3.92 \times 10^{-7}$  A. Based on the photodetector, the value is  $1.27 \times 10^{-19}$  A under the condition of 0 bias. It is much smaller than the photocurrent, which confirms that the modified photodetector has good responsiveness in ultraviolet, visible light and infrared bands.

### 3.2 Spectral response

In order to study the influence of different wavelengths on the photodetector, we investigate the responsivity of the detector at different wavelengths. Figure 4 (e) is the curve obtained with incident power of 0.1 uW and wavelength from 200 nm to 900 nm. The average response of the incident wavelength from 200 nm to 1100 nm range is about 4.78 A/W. The peak value is near 650 nm, and the response is 7.0 A/W. Comparison of the responsivity of photodetectors in the wavelength range from 450 nm to 900 nm. It can be seen from the figure that the photodetector has good responsiveness in the ultraviolet band, visible band and infrared band, which proves that the photodetector has the ability of wide spectrum detection.

The expression for responsiveness R is as follows:

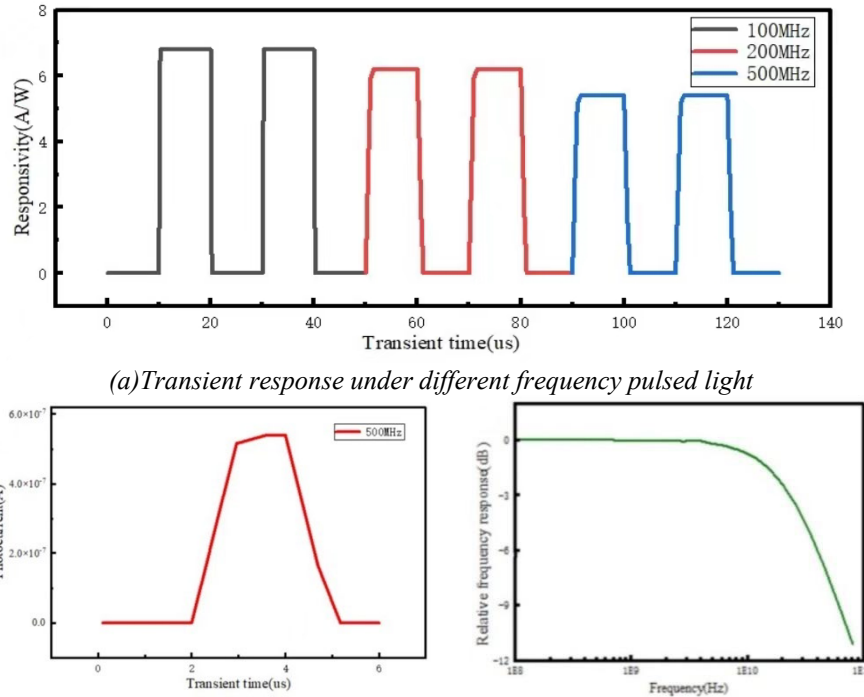
$$R_{\lambda} = I_{ph} / P_{\lambda} \quad (1)$$

$R_{\lambda}$  is the response,  $I_{ph}$  represents the composite photocurrent that is, the difference between the output photocurrent and the dark current,  $P_{\lambda}$  represents the input optical power.

### 3.3 Transient response

In order to study the response speed of the photodetector, we investigate the response of the photodetector in photovoltaic mode with a wavelength of 650 nm at different modulation frequencies. Figure 5 (a) show the transient response curves of the photodetector under different incident light frequencies under 650 nm light irradiation in photovoltaic mode. As can be seen from the figure, the optical responsiveness of 100 MHz incident light frequency is 6.8 A/W. The optical responsiveness of 200 MHz incident optical frequency is 6.2 A/W. The optical responsivity of 500 MHz incident light frequency is 5.4 A/W. Figure 5 (b) shows the transient response of the detector at modulation frequency of 500 MHz, incident light wavelength of 650 nm, and incident power of 0.1 uW. The results show that

the rise time of the photodetector is 1.59 us and the fall time is 1.10 us. Next, we study the working bandwidth of the photodetector. As can be seen from Figure 5 (c), it is found that the working 3dB bandwidth of the photodetector is as high as 23.4 GHz. In summary, the photodetector has fast response speed, wide operating bandwidth, and the ability to explore ultra-fast light.



(a) Transient response under different frequency pulsed light  
 (b) The rising time when the frequency is 500 MHz between and down time (Left)  
 (c) The frequency response of the light wavelength is 650 nm (right)

Figure 5: Transient response of PIN photodetector

### 3.4 Sensitivity

In order to evaluate the detection limit of the photodetector, we analyze the detection limit of the photodetector by simulating the equivalent noise power and the specific detection rate of the photodetector. There are three main sources of noise in photodetectors: 1/f noise, shot noise and thermal noise. [8] The main part of low frequency noise is 1/f noise. The main parts of high frequency noise are shot noise and thermal noise. [9] When the signal power is higher than the noise power, the signal can be effectively detected. The equivalent noise power can be roughly calculated using the formula 2.

$$NEP = I_N / R \quad (2)$$

Where,  $I_N$  denotes the noise current under no light condition and the bandwidth test condition is 1Hz, and R denotes the optical responsiveness.

Specific detectivity is an index to measure the performance of photodetector. It refers to the detection rate under the condition of 1Hz bandwidth in unit photosensitive area. The calculation may be made by formula 3.

$$D^* = R \sqrt{A \Delta f} / NEP \quad (3)$$

Where, A represents the photosensitive area and  $\Delta f$  represents working bandwidth.

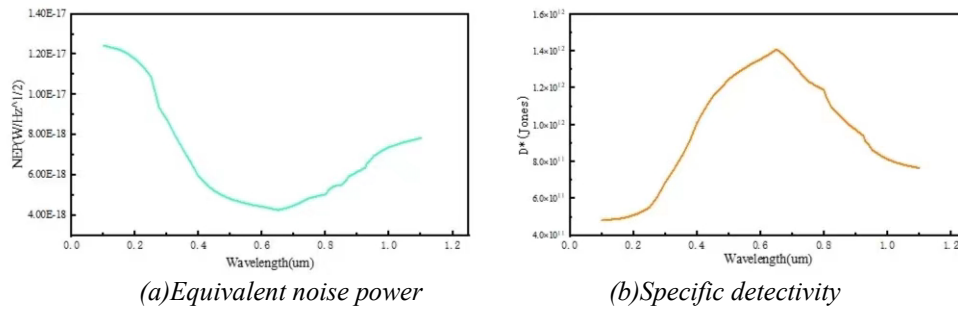


Figure 6: Sensitivity of PIN photodetector

Figure 6 (a) is the equivalent noise power of the photodetector. It can be seen from the figure that the equivalent noise power in the wavelength range of 0.1  $\mu\text{m}$  to 1.1  $\mu\text{m}$  is around the order of  $10^{-18}$  as a whole, and the photodetector has a stable detection rate in the ultraviolet region, the light-seeing region and the outer optical band. Based on the heterogeneous structure of the photodetector, the problem of lattice mismatch is not considered and the noise current is limited. The photodetector operates in photovoltaic mode, greatly reducing dark current. Visible light - red light band, detection ability is very significant. Figure 6 (b) is the curve of the specific detectivity of the photodetector as the wavelength changes. It can be seen from the figure that the specific detectivity of the photodetector in this band is stable above  $10^{11}$ , and the specific detectivity near the peak value of 650 nm is as high as  $1.4 \times 10^{12}$  Jones. It is further proved that the photodetector has high detection ability and rapid response.

#### 4. Conclusions

A PIN type photodetector is designed to solve the problem of narrow spectrum and high noise of photodetectors. Based on the excellent photoelectric characteristics of  $\text{MoS}_2$ , we designed a PIN type Schottky contact  $\text{MoS}_2/\text{Ge}$  heterojunction photodetector. Simulation results show that the photodetector has small dark current and large photocurrent, and the dark current is mainly reduced by Schottky contact. The spectral response is wide, covering the ultraviolet, visible and near-infrared regions. In addition, it has fast transient response, operating bandwidth up to 20 GHz and above, low detection limits and high detection rates. PIN-type  $\text{MoS}_2/\text{Ge}$  heterojunction photodetectors are performing well and will continue to optimize material parameters to further improve performance and support the development of photodetectors.

#### References

- [1] Wu G, Wang X, Chen Y, et al. Ultrahigh photoresponsivity  $\text{MoS}_2$  photodetector with tunable photocurrent generation mechanism [J]. *Nanotechnology*, 2018, 29(48): 485204.
- [2] Huang Z, Zhang T, Liu J, et al. Amorphous  $\text{MoS}_2$  photodetector with ultra-broadband response [J]. *ACS Applied Electronic Materials*, 2019, 1(7): 1314-1321.
- [3] Du Y, Xu Y, Huang K, et al. Design and calculation of photoelectric properties of resonance enhanced  $\text{InAs}/\text{GaSb}$  type-II superlattices photodetectors with diffraction rings structure [J]. *Heliyon*, 2024, 10(11). DOI:10.1016/j.heliyon.2024.e32543.
- [4] Gonzalez Marin J F, Unuchek D, Watanabe K, et al.  $\text{MoS}_2$  photodetectors integrated with photonic circuits [J]. *npj 2D Materials and Applications*, 2019, 3(1): 14.
- [5] Kumar R, Goel N, Raliya R, et al. High-performance photodetector based on hybrid of  $\text{MoS}_2$  and reduced graphene oxide [J]. *Nanotechnology*, 2018, 29(40): 404001.
- [6] Lin X, Wang F, Shan X, et al. High-performance photodetector and its optoelectronic mechanism of  $\text{MoS}_2/\text{WS}_2$  vertical heterostructure [J]. *Applied Surface Science*, 2021, 546: 149074.
- [7] Wang L, Chen L, Wong S L, et al. Electronic devices and circuits based on wafer-scale polycrystalline monolayer  $\text{MoS}_2$  by chemical vapor deposition [J]. *Adv Electron Mater* 2019; 5: 1900393.
- [8] Li Z, Wu J, Wang C, et al. High-performance monolayer  $\text{MoS}_2$  photodetector enabled by oxide stress liner using scalable chemical vapor growth method [J]. *Nanophotonics*, 2020, 9(7): 1981-1991.
- [9] Zhang Yuhang, Zhao Weiwei, Liu Hongwei, et al. Research progress of self-powered photodetectors based on low-dimensional materials [J]. *Acta Physico-Chimica Sinica*, 2023: 2310004.